Journal of *Marine Science and Engineering*

MDPI

Article

Emission Estimation and Spatiotemporal Distribution of Passenger Ships Using Multi-Source Data: A Case from Zhoushan (China)

Xubiao Xu [1], Xingyu Liu [2], Lin Feng [3], Wei Yim Yap [4] and Hongxiang Feng [1,*]

[1] Faculty of Maritime and Transportation, Ningbo University, Ningbo 315832, China; 2211120015@nbu.edu.cn
[2] Faculty of Governance and Global Affairs, Leiden University, 2311 EZ Leiden, The Netherlands; liuxingyu0423@gmail.com
[3] Department of Logistics and Maritime Studies, The Hong Kong Polytechnic University, Hong Kong TU428, China; 23100478d@connect.polyu.hk
[4] School of Business, Singapore University of Social Sciences, Singapore 599494, Singapore; wyyap@suss.edu.sg
* Correspondence: fenghongxiang@nbu.edu.cn

Abstract: Quantifying and estimating shipping emissions is a critical component of global emission reduction research and has become a growing area of interest in recent years. However, emissions from short-distance passenger ships operating on inter-island routes and their environmental impacts have received limited attention. This contribution investigated the temporal and spatial distribution characteristics of pollutants emitted by short-distance passenger ships at Zhoushan (China) using Automatic Identification System (AIS) data and the bottom–up emission model integrated with multi-source meteorological data. A year-long emission inventory was investigated. The results indicated that high-speed passenger ships contributed to the largest share of the emissions. The emissions were predominantly concentrated during daytime hours, with the routes between Zhoushan Island and Daishan, Daishan and Shengsi, and Zhoushan Island and Liuheng Island accounting for most of the emissions. Furthermore, intra-port waterways were identified as the primary emission areas for short-distance passenger ships. This study provides essential data support and references for the relevant authorities to understand the emission patterns of short-distance passenger ships, thereby facilitating the formulation of targeted emission reduction strategies for the maritime passenger transport sector.

Keywords: emission estimation; spatiotemporal distribution; automatic identification system (AIS) data; passenger ship; bottom–up emission model

Academic Editor: Rose Norman

Received: 13 December 2024
Revised: 6 January 2025
Accepted: 13 January 2025
Published: 18 January 2025

Citation: Xu, X.; Liu, X.; Feng, L.; Yap, W.Y.; Feng, H. Emission Estimation and Spatiotemporal Distribution of Passenger Ships Using Multi-Source Data: A Case from Zhoushan (China). *J. Mar. Sci. Eng.* **2025**, *13*, 168. https://doi.org/10.3390/jmse13010168

1. Introduction

Maritime activities play a vital role in global exhaust emissions, and the atmospheric pollutants associated with these activities have become significant concerns at both the regional and global levels [1–3]. With increasing attention on climate change, the international community has imposed stricter regulatory requirements on greenhouse gas emissions from the shipping industry. For instance, the International Maritime Organization (IMO) has established carbon emission standards for global shipping and encouraged the adoption of environmentally friendly fuels and technologies, aiming to mitigate global warming by reducing carbon dioxide emissions [4–6]. Some countries have also initiated remote monitoring programs to effectively enforce emission policies and regulations [7,8]. Consequently, the governance of ship emissions has become a critical focus of global regulations.

Effective emission governance requires the support of policy and regulatory measures, and the development of ship emission inventories, which contain data on atmospheric and greenhouse gas emissions as well as their spatial distribution, is crucial to forming the foundation for such actions [9,10]. Most past research on ship emissions has primarily focused on global or regional maritime traffic, particularly emissions from large merchant ships. Although the per-ship emissions of short-distance passenger ships are relatively small, their high frequency of operations, short voyages, and routes located in densely populated coastal areas make their emissions highly impactful on local air quality. These emissions have a direct effect on the health of island and coastal residents [11]. However, studies assessing the environmental and socio-economic impacts of emissions from small passenger ships operating on inter-island routes or ferries navigating urban ports remain insufficient. A key issue is that previous emission inventories have rarely considered short-distance passenger ships within specific regions, resulting in gaps in targeted emission control strategies [12]. Therefore, there is an urgent need to conduct an assessment of the impact of passenger ship emissions in areas such as island cities and island regions where passenger ships sail densely. This led to our research topic: quantifying the pollutant emissions of short-distance passenger ships in the target area, with a particular focus on their spatial and temporal distribution characteristics.

According to IMO regulations [13], all ships with a 300 Gross Tonnage or above engaged in international voyages, cargo ships with a 500 Gross Tonnage or above not engaged in international voyages, and all passenger ships must be equipped with AIS devices. AIS is a navigational system designed to enhance maritime safety and communication between ships and the shore or between ships. It plays a crucial role in maritime services, such as reducing ship collision incidents. AIS data are automatically exchanged at high frequencies between ships and shore stations and recorded, providing geographic information with high temporal precision for ship emission studies. All passenger ships operating within Chinese waters must be equipped with AIS devices, enabling the acquisition of high-precision operational data for short-distance passenger ships with frequent voyages, thereby supporting the development of emission inventories.

The contributions of this research is twofold. First, we propose a framework for estimating emissions from short-distance passenger ships using multi-source data (i.e., AIS data, attribute data, and meteorological and environmental data) and the bottom–up emission model. Secondly, the spatiotemporal characteristics of passenger ship emissions in Zhoushan, China, were investigated and a one-year-long emission inventory was established.

The remainder of this paper is structured as follows: Section 2 reviews the relevant literature; Section 3 outlines the research questions; Section 4 details the methodology, including the model construction and data-processing steps; Section 5 presents an empirical study of short-distance passenger ships in Zhoushan, China; and finally, Section 6 summarises the most important findings.

2. Literature Review

Traditional methods for calculating emission inventories mainly include top–down and bottom–up approaches [14,15]. The top–down method starts from macro-level statistical data, such as fuel consumption and shipping activities, and calculates emissions by multiplying fuel consumption by emission factors [16]. Although simple and efficient in producing emission inventory results, this method may lack the level of detail needed for micro-level analyses due to its broader assumptions and its limited consideration of the actual movement of ships. However, it remains highly effective and accurate for global- or regional-scale studies [17]. In contrast, the bottom–up method can provide more accurate

emission estimates for finer-scale analyses [18,19]. It estimates emissions by considering the operational status, engine power, fuel consumption, and corresponding emission factors of ships to calculate emissions for each interval between two consecutive AIS positions [20]. Jalkanen et al. [21] first developed the STEAM (Ship Traffic Emission Assessment) model for ship emissions, using AIS data to calculate pollutant emissions from ships in the Baltic Sea, and constructed an emission inventory. Following this, many studies utilised AIS data to compile emission inventories [22–25]. Chen et al. [26] created a high temporal and spatial resolution emission inventory for ships in China for 2014, filling a gap in the national emission inventory. Toscano et al. [27] developed an emission inventory for the Port of Naples based on 2018 data, assessing its impact on air quality at an urban scale. Ye et al. [28] used emission inventories from 13 case studies, comparing river–sea hybrid models, river–sea models, and mixed models using a bottom–up approach. Li et al. [29] proposed a spatiotemporal STSD iterative correction model based on a random forest algorithm and an ST–DBSCAN-based trajectory segmentation algorithm to estimate CO_2 emissions from ships in China's domestic emission control areas (DECAs). This method is also commonly applied to emission studies of ships in inland river basins. Zhi et al. [30] compiled a 2019 greenhouse gas inventory for China, illustrating the relationship between economic development and emissions. The bottom–up method is particularly suitable for understanding the emission levels of individual ships or specific ship types, such as emissions on particular routes or at ports. Still, it requires a large volume of research data. The influence of meteorological factors on ship emissions has also gained attention, reducing uncertainties in emission models [31]. Moreno-Gutiérrez and Durán-Grados [32] proposed the SENEM model (Ship's Energy Efficiency Model), which, compared to the STEAM model, considers real-time power adjustments influenced by wind, waves, and currents. Studies have consistently shown that bottom–up methods considering operational states are more accurate and have been widely applied to calculate emissions from ships in global waters and port areas.

While numerous studies have explored and calculated ship emission inventories and their impacts, the research gap on short-distance passenger ships still needs to be filled. Significant emissions from large ships have been the primary focus of researchers, with emission calculations typically considering auxiliary engines and boilers. The established emission inventories often include only partial emissions from passenger ships in port areas. Carić et al. [33] assessed the environmental burdens of cruise ships at Croatian ports, highlighting potential human ecological risks, with cruise ships identified as a notable emission source. Dragović et al. [34] investigated cruise ship traffic and found that factors such as berth availability and accessibility, in addition to marine fuel, influence emission levels. Chen et al. [35] studied the activities of passenger ships in the Arctic, revealing adverse impacts on the marine ecosystem and analysing CO_2 emissions under different fuel options, suggesting liquefied natural gas (LNG) as a better choice. Additionally, Chen et al. [36] analysed the impact of COVID-19 on passenger ships in Danish waters, finding significant effects on cruise ships but minimal impact on ferries. For small passenger ships, the research has primarily focused on ferry emissions [37]. Chou et al. [38] estimated the CO_2 emissions of ferries operating on urban port routes and nearby island routes in Taiwan using the Energy Efficiency Index and proposed potential emission reduction policies. Mannarini et al. [39] used a mixed-effect linear model to analyse ferry emissions in the European Economic Area from 2018 to 2020, characterising the impact of COVID-19 on ferry emissions and evaluating the causality between the pandemic and pollutant emissions. Baird and Pedersen [40] calculated the CO_2 emissions from short- and long-distance ferries operating between mainland Scotland and the Orkney Islands, concluding that the optimal solution for medium-sized ferries serving islands is to use or develop

the shortest maritime routes to minimise CO_2 emissions from transportation. To optimise emissions, researchers have also explored fuel alternatives for ferries to reduce pollutant emissions [41–43]. However, the results indicate that internal combustion engines remain the dominant hybrid power source, and emissions from short-distance passenger ships require continued attention in the short term. Thus, comprehensive regional evaluations of short-distance passenger ship emissions remain necessary in the absence of alternative power sources.

In summary, bottom–up methods based on dynamic AIS data, which fully consider the operational status of ships and provide precise data for passenger ship emissions, offer higher transparency and traceability compared to model estimates or indirect calculations. This enhances the credibility and reliability of research findings, making them more suitable for calculating emissions from passenger ships. Most studies, however, have concentrated on total emissions from global ocean-going ships or general emissions from port areas [44,45]. Previous research on passenger ship emissions has primarily focused on long-distance recreational cruises and short-distance ferries. In contrast, emissions from short-distance passenger ships operating inter-island routes for transportation purposes require targeted study.

Overall, although emissions from short-distance passenger ships have a relatively smaller global impact compared to ocean-going ships, their high-frequency operations in specific regions significantly affect local environments. This study adopted a bottom–up approach based on dynamic AIS data to estimate and analyse the spatiotemporal characteristics of short-distance passenger ship emissions, uncovering their emission patterns and environmental impacts.

3. Problem Description

Short-distance passenger ships operate according to publicly available schedules, navigating between inter-island passenger terminals and along designated routes specified by regulatory authorities. Although many emission inventories include data on passenger ships, the construction and operation of short-distance passenger ships differ significantly from larger ships such as cruise ships. Previous studies often estimated emissions based on the default main engine power, which likely led to the underestimation of the actual emissions [46].

3.1. Characteristics of Short-Distance Passenger Ships

The development of emission inventories for short-distance passenger ships requires an in-depth understanding of their characteristics. Short-distance passenger ships have the following operational characteristics. First, they are equipped with specialised passenger terminals to facilitate ticket purchases and boarding for residents, which differs from larger ships that dock at general-purpose port berths. Second, their primary purpose is to serve the transportation needs of residents in nearby island regions. These ships are constructed to carry passengers and vehicles, with significant variations in engine power depending on the type and quantity of transported objects as well as the operational purpose of the ship. Since these ships operate exclusively within designated areas, regulatory authorities impose strict schedules for departure, navigation, and berthing.

3.2. Operating Modes of Short-Distance Passenger Ships

According to the definitions in previous emission inventories, the operational modes of large ships can be categorised based on their speed and location [47]. However, the operational modes of short-distance passenger ships differ and can be defined as berthing, unberthing, and cruising. Unlike large ships, idling at berth is not considered for passenger

ships since auxiliary engines and boilers are not operational during berthing, and no emissions are generated. The detailed definitions of these operational modes are as follows:

- Berthing: Short-distance passenger ships enter the passenger terminal area from open water, gradually reducing their speed to ensure a safe and stable docking at the designated berth.
- Unberthing: The ship slowly departs from the terminal berth, gradually adapting to navigation conditions in open water.
- Cruising: In this mode, the ship sails along a predetermined route in open water, maintaining a steady speed to ensure a comfortable experience for passengers.

Taking a Roll-on/Roll-off (Ro-Ro) passenger ship as an example, its berthing process, as shown in Figure 1a, involves a gradual deceleration as it approaches the terminal. Around 8:15, the ship's speed decreases from approximately 10 knots to around 3 knots, reducing its kinetic energy to facilitate safe berthing. During this approach, operators adjust the ship's heading based on the wind direction, tidal currents, and other factors, ensuring alignment with the designated berth. Once the alignment is complete, the ship further reduces its speed to below 2 knots, moving slowly into the berth. For unberthing, the ship is carefully unberthed away from the berth at a speed typically below 3 knots, as shown in Figure 1b. Once clear of the berth, operators adjust the ship's heading according to the departure plan, allowing it to transition smoothly to its designated route.

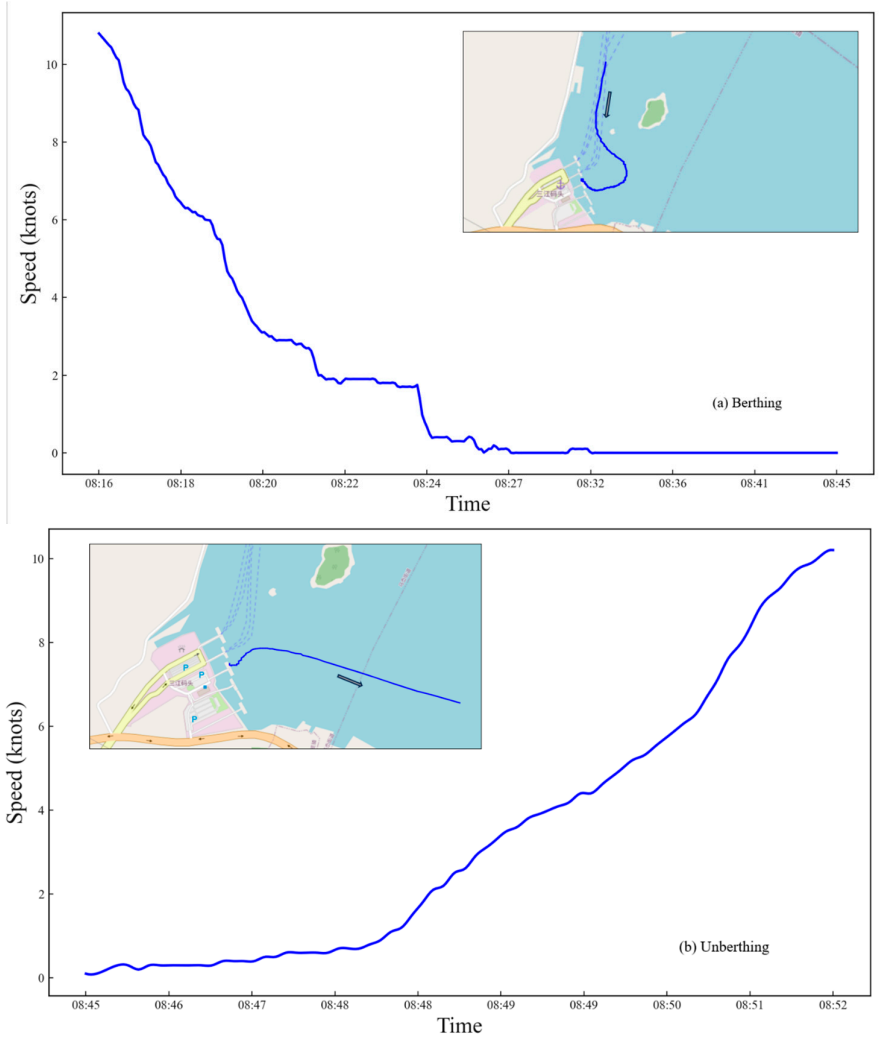

Figure 1. Berthing (**a**) and unberthing (**b**) process of a passenger ship.

4. Methodology

The overall technical workflow of this study is shown in Figure 2. It primarily includes the processing, calculation, and visualisation of the AIS-based ship emission inventory, which consists of five main steps. First, the AIS data underwent pre-processing, including cleaning abnormal information and identifying Maritime Mobile Service Identities (MMSIs) corresponding to passenger ships or high-speed ships, followed by matching the relevant dynamic details. Second, the technical specifications of passenger ships were collected, and corrections to the ship speeds were made based on meteorological factors. Third, the key parameters were determined, including the actual operating speed of the ship, emission factors, main engine load coefficients, as well as the ship's emission location and time stamps. Fourth, the pollutant emissions from passenger ships' main engines were calculated to generate an emission inventory. Finally, visualisation software was used to create spatial distribution maps of the pollutant emissions.

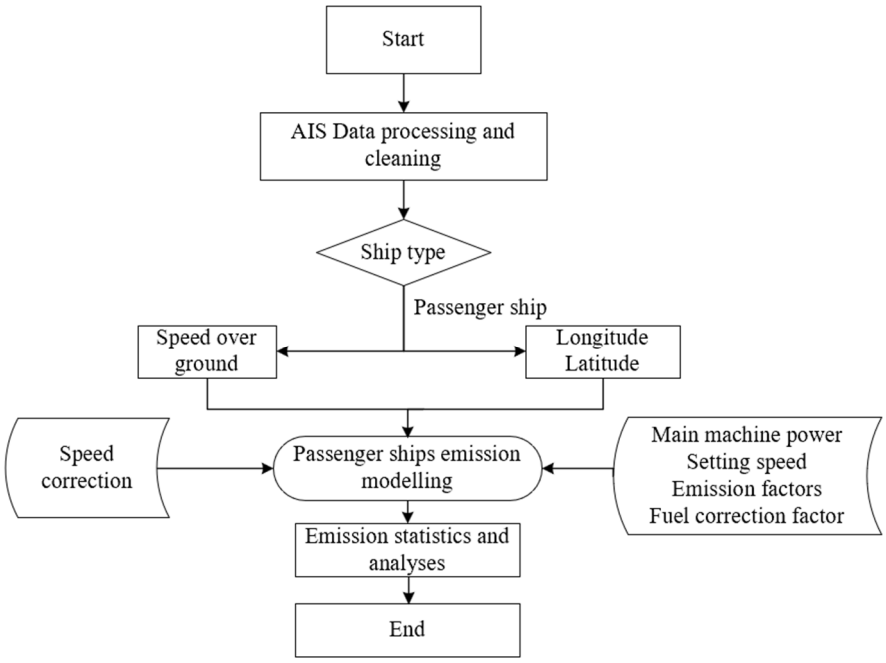

Figure 2. Logic framework.

4.1. Identification Algorithm for Berthing and Unberthing Operations

The identification of operational modes during the berthing and unberthing processes of short-distance passenger ships is a critical foundation for quantifying ship pollutant emissions. This study built upon the algorithm proposed by Chen et al. [48], employing a trajectory-based recognition algorithm. Analysing key parameters such as ship position and speed, the algorithm achieves precise localisation of berthing and unberthing processes. The core of this algorithm lies in constructing a multi-parameter recognition model that integrates ship trajectories, speed variations, and the spatial characteristics of passenger terminals. First, an AIS dataset Si for passenger ships in the terminal area is collected, and complete trajectory information is extracted. Then, based on key parameter definitions, including the distance threshold d and the speed range $(\underline{v}, \overline{v})$, a refined identification of berthing and unberthing behaviours is conducted. The implementation process is detailed in Algorithm 1.

Algorithm 1 identifies the berthing and unberthing processes of the passenger ships based on trajectory characteristics. The first step involves extracting the trajectory subset Si between the passenger terminal and the berth or vice versa and conducting an initial screening. The second step identifies a collection of continuous low-speed or stationary

points approaching the berth, based on predefined distance thresholds and speed ranges, which are marked as the berthing trajectory point set. Subsequently, by detecting trajectory segments where the ship's speed gradually increases and moves away from the berth, the unberthing trajectory point set is further extracted. Using this method, we can identify the berthing and unberthing modes of passenger ships.

Algorithm 1. Framework algorithm for estimating emissions from passenger ships.

Step 1: For the short distance passenger ships trajectory data*set* ***i*** extract the dataset ***Si*** between the passenger terminal boundary to the berth or the berth to the passenger terminal boundary.
Step 2: Determine if the passenger ship trajectory in the ***Si*** data satisfies the following two conditions: i. The speed of the passenger ship trajectory point is between v_{-} **and** $\overline{v}$. ii. The distance between the passenger ship and the pier is less than ***d*.**
Step 3: The trajectory points in the trajectory dataset ***Si*** that continuously approach the terminal are used to construct a set of continuous low-speed\stationary points, which are recorded as the berthing trajectory point set.
Step 4: Detect the changes in the speed and position of the passenger ships in the berthing area. If there are trajectory points that continuously move away from the terminal and the speed gradually increases to $\overline{v}$, this segment of the trajectory is recorded as the unberthing trajectory point set. Step 5: Repeat steps 1–4 to obtain a passenger ship berthing (unberthing) dataset.

4.2. Estimating Emissions of Main Engines

This study adopted a bottom–up approach based on AIS data to calculate the emissions of pollutants such as carbon dioxide (CO_2), nitrogen oxides (NO_x), carbon monoxide (CO), particulate matter ($PM_{2.5}$ and PM_{10}), and sulphur dioxide (SO_2) from passenger ships. The short-distance passenger ships studied here are powered by dual main engines and are not equipped with auxiliary engines or boilers. Thus, the emission calculation in this study focused solely on the main engines. The methodology first estimates the emissions for each trajectory segment between two consecutive AIS messages using the bottom–up calculation approach. These segment-level emissions are then summed to obtain the total emissions of a single ship. Finally, the emissions of all ships in the study region are aggregated. This approach is represented mathematically as Equation (1):

$$E_{m,i,j} = P_m \cdot LF \cdot T_j \cdot EF_{m,i} \cdot LLA \cdot 10^{-6} \quad (1)$$

where

$E_{m,i,j}$ is the emissions of ship i in trajectory segment j (tons);

P_m is the main engine power of the ship (kW);

LF is the load factor of the main engine (dimensionless);

T_j is the running time of trajectory segment j(h);

$EF_{m,i}$ is the emission factor of pollutant i for main engine m (g/kWh);

LLA is the emission adjustment factor, which is equal to 1 if LF is greater than 20% and adjusted otherwise.

$$E_{m,i} = \sum_{j=1}^{N_i} E_{m,i,j} \quad (2)$$

where

$E_{m,i}$ is the total emissions from ship i (tons);

N_i is the total number of trajectory segments of ship i.

$$E = \sum_{i=1}^{M} E_{m,i} \tag{3}$$

where

E is the total emissions of all ships in the study area (tons);
M is the total number of ships in the study area.

4.2.1. Engine Power

The load power of the ship's main engine refers to the actual power output of the main engine during operation, while the rated power of the main engine is the maximum power needed to continuously produce underrated speed and normal maintenance cycles, without external environmental influence. Variations in the power model have a relatively high impact on emission estimations.

In previous studies, researchers have typically extracted data on main engine power characteristics from databases such as the Lloyd's Register, CCS, or IMO database. However, accessing comprehensive local ship databases globally often presents challenges. Many existing studies have attempted to address this data gap by using models to predict missing entries related to ship technical specifications [49]. This approach introduces certain inaccuracies and is one of the largest sources of uncertainty in AIS data-based methods [50,51]. For the short-distance passenger ships under investigation, we adopted a more comprehensive and rigorous data collection strategy to obtain key technical parameters, particularly main engine power. This strategy significantly reduces the amount of missing data and enhances the accuracy of emission calculations.

4.2.2. Emission Factors

Emission factors (EFs) are empirical parameters whose selection is directly related to the engine type, fuel type, and sulphur content, and they are influenced by various external factors [52]. Engines are categorised by speed into slow-speed diesel (SSD) engines and medium-speed diesel (MSD) engines. They are further classified by fuel types, such as heavy fuel oil (HFO), marine diesel oil (MDO), and marine gas oil (MGO). This study used the emission factors recommended under different circumstances by Entec UK Limited [53] and the Starcrest Consulting Group [54], as outlined in Table 1. It is important to note that these studies were based on marine diesel oil with a sulphur content of 0.5% and heavy fuel oil with a sulphur content of 2.7%. For fuels with differing sulphur contents, this study applied specific fuel correction factors to ensure the accuracy and applicability of the emission factors. The specific correction values are detailed in Table 2. The correction factors for the sulphur content were derived from established guidelines and validated through empirical studies. These factors used to adjust the emission estimates to account for variations in fuel sulphur contents. While they improve the accuracy of the estimates, it is important to acknowledge that the sulphur content of fuel may vary across batches and operational conditions, which could introduce uncertainties into the calculations.

Table 1. Emission factors [52,53] (unit: g/kWh).

Machine Type	Engine Type	Fuel Type	Built Year	CO_2	CO	HCs	NO_x	SO_2	$PM_{2.5}$	PM_{10}
ME	MSD	MDO	<1999	649	1.1	0.5	13.2	2.1	0.35	0.38
ME	MSD	MDO	2000–2010	649	1.1	0.5	12.2	2.1	0.35	0.38
ME	MSD	MDO	2011–2015	649	1.1	0.5	10.5	2.1	0.35	0.38
ME	MSD	HFO	<1999	683	1.1	0.5	13	11.5	1.2	1.5
ME	MSD	HFO	2000–2010	683	1.1	0.5	14	11.5	1.2	1.5
ME	MSD	HFO	2011–2015	683	1.1	0.5	11.2	11.5	1.2	1.5

Note: ME refers to the main engine. MSD refers to medium-speed diesel. MDO refers to marine diesel oil. HFO refers to heavy fuel oil.

Table 2. Fuel correction coefficient [55].

Fuel Type	Sulphur Content (%)	CO_2	CO	HCs	NO_x	SO_2	$PM_{2.5}$	PM_{10}
MDO	0.50	1.00	1.00	1.00	0.94	0.18	0.25	0.25
MDO	0.10	1.00	1.00	1.00	0.94	0.04	0.17	0.17

4.2.3. Vessel Speed Correction

Due to the smaller size and scale of short-distance passenger ships, external factors can lead to speed losses [56]. The speed shown in AIS data generally refers to the ship's speed over ground, which already accounts for the influence of external factors such as the wind, current, and waves. To better approximate the actual operating conditions of passenger ships and improve the accuracy of emission estimates, it is necessary to correct the speed over ground to obtain the ship's true output speed. The actual speed of a ship under the influence of wind, waves, and currents is equal to the speed provided by AIS data minus the wind-induced drift speed, current-induced drift speed, and wave-induced drift speed. The speed correction method proposed by Huang et al. [57] was adopted, with the process detailed below.

The wind, wave, and current data used in this study were sourced from the Copernicus Marine Environment Monitoring Service (CMEMS). First, the combined influence of wind and currents on the ship's speed is corrected. Assuming that the ship's pre-affected speed is $\vec{V}_{oss}$, it can be calculated using Equation (4):

$$\vec{V}_{sog} = \vec{V'}_{oss} + \vec{V}_{wnd} + \vec{V}_{cur} \tag{4}$$

Through orthogonal decomposition, Equation (4) can be rewritten as

$$\begin{cases} u_{sog} = \vec{V'}_{oss} + \vec{V}_{cur} * cos\theta_{ct} - \vec{V}_{wnd} * cos\theta_{wt} \\ v_{sog} = \vec{V}_{cur} * sin\theta_{ct} - \vec{V}_{wnd} * sin\theta_{wt} \\ \vec{V}_{sog} = \sqrt{{u_{sog}}^2 + {v_{sog}}^2} \end{cases} \tag{5}$$

where

$\vec{V}_{sog}$ is the speed over ground;

$\vec{V'}_{oss}$ is the engine output speed after the reductions;

$\vec{V}_{wnd}$ is the wind-induced drift speed;

$\vec{V}_{cur}$ is the current speed;

u and v are the rectangular components of the speed;

θ_{ct} is the flow angle between $\vec{V}_{oss}$ and $\vec{V}_{cur}$ at time t;

θ_{wt} is the relative azimuth between $\vec{V}_{org}$ and $\vec{V}_{wnd}$ at time t.

By further processing this formula, a detailed expression for $\vec{V}_{oss}$ can be derived:

$$\vec{V}'_{oss} = \sqrt{\vec{V}_{sog}^{\,2} - \left(\vec{V}_{cur}\sin\theta_{ct} - \vec{V}_{wnd}\sin\theta_{wt}\right)^2} - \vec{V}_{cur}{*}\cos_{\theta_{ct}} + \vec{V}_{wnd}{*}\cos_{\theta_{wt}} \quad (6)$$

Finally, the influence of wave factors is corrected to obtain the original speed output of the ship's engine, $\vec{V}_{org}$, as shown in Equation (7):

$$\vec{V}_{oss} = \frac{\vec{V}'_{oss} + (K_1 + K_2h^2 - K_3qh)G}{1 + (K_1h + K_2h^2 - K_3qh)K_4D} \quad (7)$$

where

h is the effective wave height;

q is the relative azimuth;

D is the actual displacement of the ship;

K_1, K_2, K_3, and K_4 are the ship performance parameter values (K_1 = 0.745, K_2 = 0.05015, K_3 = 0.0045, K_4 = 1.35*106);

G is the empirical coefficient that is dependent on ship displacement D:

$$G = \begin{cases} 1.0 & D \le 10,000t \\ 1.09 & 10,000t < D \le 20,000t \\ 1.19 & 20,000t < D \le 40,000t \\ 1.29 & 40,000t < D \le 60,000t \end{cases} \quad (8)$$

The above model enables the calculation of ships' true engine output speed in the given AIS data and provides information about the wind, waves, and currents in the sailing area.

4.2.4. Load Factors

The load factor (LF) of a ship's main engine is a critical parameter in emission calculations. The relationship between the main engine load and ship speed can be approximately described using the propeller law [58]. Under constant sailing conditions, the ratio of the ship speed to the main engine's rotational speed typically remains unchanged. Thus, the formula for calculating the load factor is as follows:

$$LF = (\vec{V}_{org}/V_{max})^3 \quad (9)$$

where $\vec{V}_{org}$ is the actual output speed of the ship and V_{max} is the design maximum speed of the ship.

In real-world passenger transport operations, the number of passengers and vehicles carried per voyage varies, introducing uncertainty into the load factor of passenger ships. When the engine load of the main engine falls below 20%, there is a tendency for emission factors to increase as the load decreases. This is because diesel engines operate less efficiently at low loads, resulting in incomplete combustion. Therefore, these emission factors should be adjusted as a function of engine load. When the main engine load is less than 20%, a low-load adjustment factor (LLA) must be applied, as detailed in Table 3.

Table 3. Low-load adjustment factor for main engines.

Load	NO_x	SO_2	$PM_{2.5}$	PM_{10}	CO	CO_2	HCs
1%	11.47	5.99	19.17	19.17	19.32	5.82	59.28
2%	4.63	3.36	7.29	7.29	9.7	3.28	21.18
3%	2.92	2.49	4.33	4.33	6.49	2.44	11.68
4%	2.21	2.05	3.09	3.09	4.86	2.01	7.71
5%	1.83	1.79	2.44	2.44	3.9	1.76	5.61
6%	1.6	1.61	2.04	2.04	3.26	1.59	4.35
7%	1.45	1.49	1.79	1.79	2.8	1.47	3.52
8%	1.35	1.39	1.61	1.61	2.45	1.38	2.95
9%	1.27	1.32	1.48	1.48	2.18	1.31	2.52
10%	1.22	1.26	1.38	1.38	1.97	1.25	2.2
11%	1.17	1.21	1.3	1.3	1.79	1.21	1.96
12%	1.14	1.18	1.24	1.24	1.64	1.17	1.76
13%	1.11	1.14	1.19	1.19	1.52	1.14	1.6
14%	1.08	1.11	1.15	1.15	1.41	1.11	1.47
15%	1.06	1.09	1.11	1.11	1.32	1.08	1.36
16%	1.05	1.07	1.08	1.08	1.24	1.06	1.26
17%	1.03	1.05	1.06	1.06	1.17	1.04	1.18
18%	1.02	1.03	1.04	1.04	1.11	1.03	1.11
19%	1.01	1.01	1.02	1.02	1.05	1.01	1.05
20%	1	1	1	1	1	1	1

5. Case Study

5.1. Study Area

Zhoushan is China's fourth largest island (main island) and the largest archipelago, comprising 2085 islands, of which, approximately 105 are inhabited. The region experiences a high level of passenger ship activity. For islands far from the mainland, passenger ships serve as an essential mode of transportation for residents travelling to and from the islands. These ships also fulfil the role of transport vessels, delivering essential supplies to residents.

In this study, we focused on the Zhoushan Port area in Zhejiang Province, China, as the research region. The study area extends northward to Huaniao Town in Shengsi County, Zhoushan, eastward to the Dongji Islands, and southward to the Jiushan Archipelago in Xiangshan County, Ningbo. Using AIS data from the entire year of 2020, we calculated and analysed the pollutant emissions of passenger ships throughout this region. Additionally, we examined the temporal and spatial characteristics of passenger ship emissions within the study area. The research area is shown in Figure 3, which highlights several major passenger terminals.

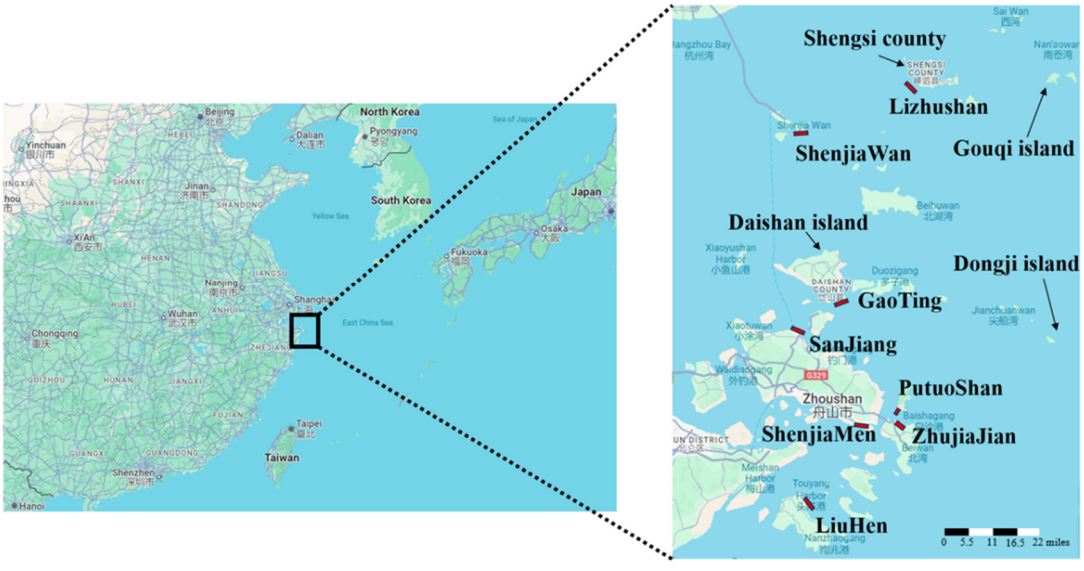

Figure 3. Map of the study area.

5.2. AIS Data

The AIS data used in this study were obtained from the East China Sea Navigation Support Center. Each daily file contained more than 10 million records. Combining the static and dynamic information provided by the AIS data is essential to accurately establish the emission inventory of passenger ships. The static ship information included MMSI (Maritime Mobile Service Identity), ship type code, IMO number, call sign, ship dimensions, estimated time of arrival (ETA), and destination. The dynamic ship information included the timestamp for data transmission and reception (UTC), MMSI, navigational status, rate of turn (ROT), speed over ground (SOG), the ship's latitude and longitude, course over ground (COG), and true heading (HDG), among others [59,60]. It is important to note that ship type codes, which ranged from 60 to 69, represent passenger ships, while codes from 40 to 49 indicate high-speed ships. Some high-speed ships also operate as passenger ships.

5.3. Passenger Ship Characteristics

From the AIS data of one year, we identified 576 ships with type codes classified as passenger ships or high-speed ships. After individually excluding ships with incorrect type codes or those not registered in the Zhoushan area, we identified 153 short-distance passenger ships operating within the study area. Based on the cargo they carry and their operational purposes, these passenger ships were categorised into four types: ordinary passenger ships, Ro-Ro passenger ships, high-speed passenger ships, and car–passenger ferries. The data for these ships were obtained from local passenger transport companies, and the average construction specifications for each type of passenger ship are shown in Table 4. Generally, all types of passenger ships use HFO during their voyages. However, car–passenger ferries differ in that they use MDO while in port and during the 15 min before and after entering or leaving the port, but switch to HFO during open-sea navigation. In the emission calculations, the corresponding emission factors were selected based on the built year, engine type, fuel consumption, and sailing characteristics of each ship.

Table 4. Passenger ship construction specifications.

Ship Type	Average Gross Tonnage	Average Main Engine Power (kW)	Average Passenger Capacity (Person)
Ordinary passenger ship	488.4	994.3	370.4
Ro–Ro passenger ship	1913.9	1902.8	337.2
High-speed passenger ship	215.4	1936	149.6
Car–passenger ferry	308.4	356.4	106.4

5.4. Passenger Ship Trajectory Distribution in the Zhoushan Area

Figure 4 illustrates the trajectory distribution of passenger ships in the Zhoushan area from January to December 2020. The complex trajectory map reflects the frequent movements of ships between the various islands. It can be observed that ordinary passenger ships primarily operated between Zhujiajian Island, Dongji Island, and Shengshan–Gouqi Island on the eastern side, as well as between Shengsi Island and Shenjia Wan. These ships are responsible for transporting passengers over relatively long distances. Ro-Ro passenger ships and high-speed passenger ships mainly navigated between Zhoushan Island, Liuheng, and Daishan. Ferries, on the other hand, were primarily used for short-distance transportation and were seen operating between closely located islands. The most densely trafficked areas were concentrated near Daishan Island, Putuo Island, and Zhoushan Island, where passenger ships frequently entered and left the ports. These locations served as key hubs for docking and transit operations.

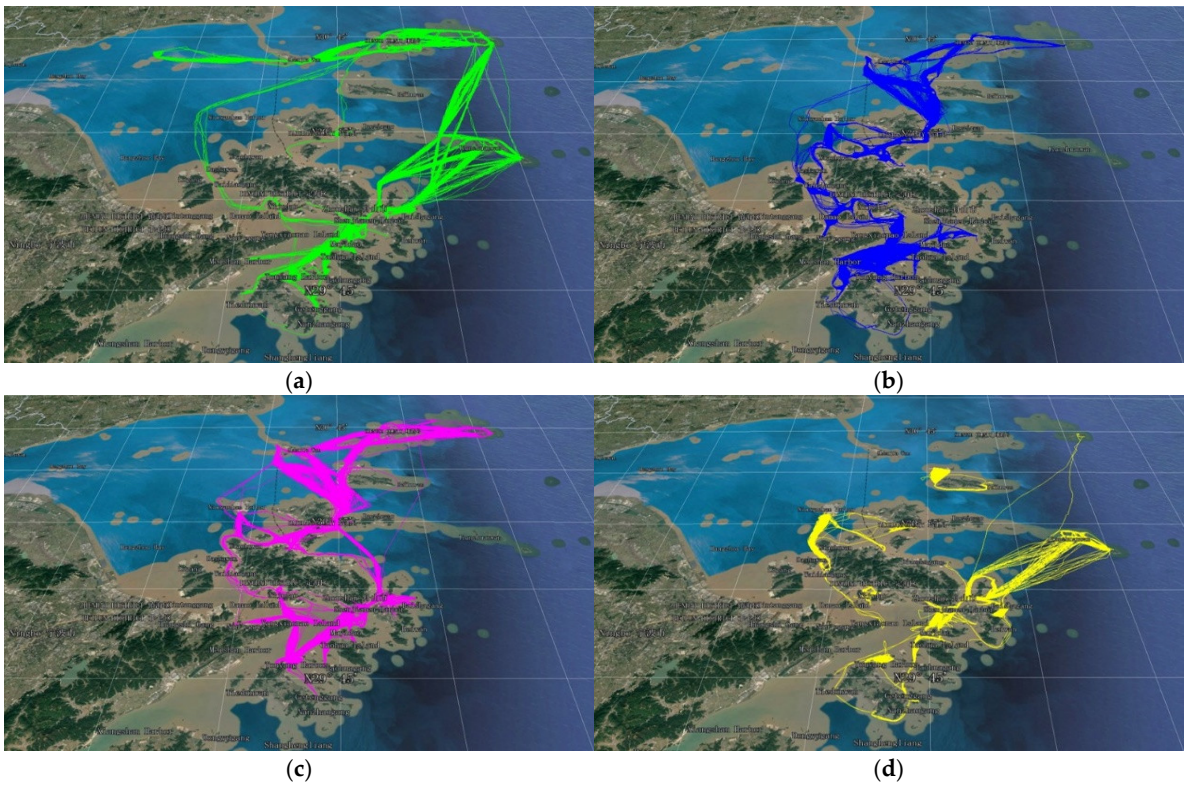

Figure 4. Passenger ship trajectory distribution in Zhoushan area. (Green for ordinary passenger ships, blue for Ro-Ro passenger ships, red for high-speed passenger ships, and yellow for ferries). (**a**) Ordinary passenger ships, (**b**) Ro-Ro passenger ships, (**c**) high-speed passenger ships, and (**d**) ferries.

5.5. Emission Results

Although 2020 was influenced by the COVID-19 pandemic, our analysis suggests that the primary trends and patterns in emissions remained consistent with the objectives of this study. Using the atmospheric pollutant emission model for passenger ships, the emissions of major pollutants in the Zhoushan area were calculated. The results for the total emissions were as follows: 54,895.75 tons for CO_2, 1057.82 tons for NO_x, 101.46 tons for CO, 7.68 tons for $PM_{2.5}$, 8.33 tons for $PM_{2.5}$, 32.02 tons for SO_2, and 50.34 tons for HCs.

5.6. Temporal Features of Emission Inventory

5.6.1. Temporal Distribution

The monthly variation in emissions for the different pollutants is shown in Figures 5 and 6. It could be observed that the emissions in February are significantly low with a narrower and more concentrated distribution. This was attributable to the Chinese Lunar New Year in January and February 2020, as well as the COVID-19 pandemic. The pandemic control measures led to the suspension of most passenger ship operations during this period. The peak monthly emissions of passenger ship pollutants occurred in mid-August and early October. This was likely related to increased passenger traffic during the summer season. As passenger ships are essential for reaching the islands, their operational frequency and load increased during this time, contributing to the highest emissions. In contrast, the emissions in November and December showed consecutive declines, with reductions of 16.3% and 10.5%, respectively, compared to the previous months. We speculate that this decrease was due to seasonal changes and lower temperatures, which reduce the demand for leisure travel, leading to a corresponding decline in emissions.

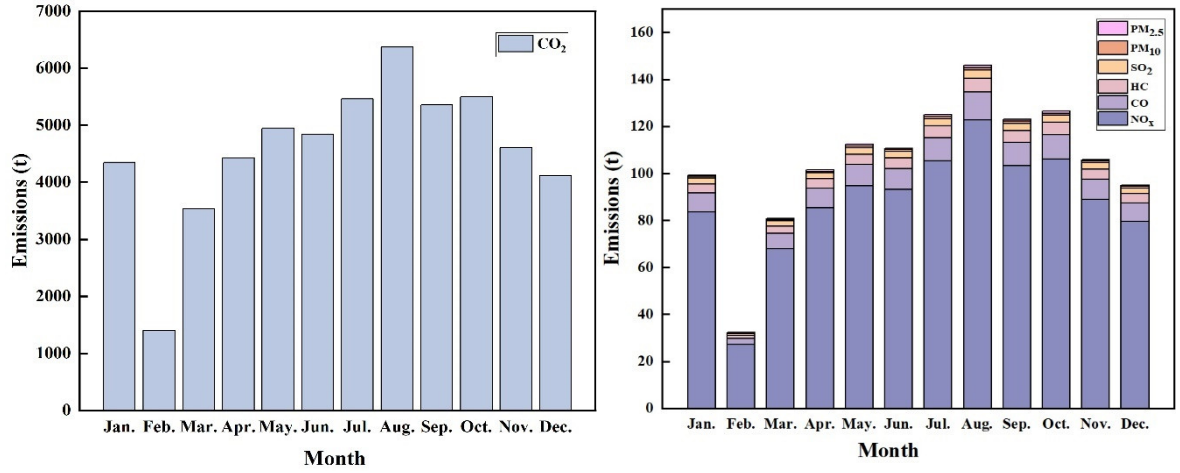

Figure 5. Variation in emissions of individual pollutants over the year (CO_2 on the **left**, other pollutants on the **right**).

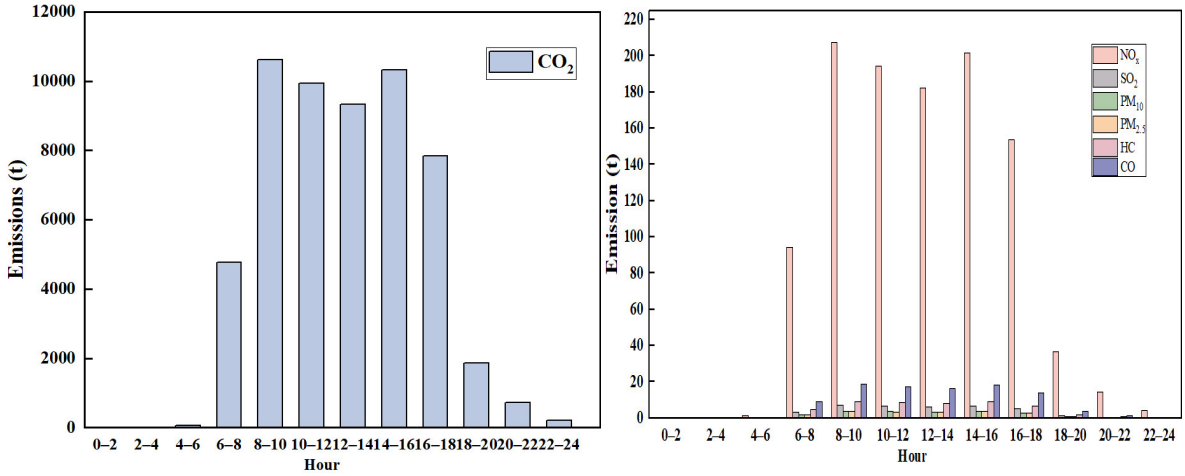

Figure 6. Distribution of emissions throughout the day (CO_2 on the **left**, other pollutants on the **right**).

To further analyse the temporal distribution of the emissions, the data were divided into 12 two-hour intervals, allowing for a detailed examination based on the time of day. Figure 6 illustrates the differences in the emissions across these intervals. The period from 08:00 to 10:00 recorded the highest emissions, with CO_2 emissions reaching 10,402.85 tons. Additionally, 10:00–12:00 and 14:00–16:00 represented two other peak emission periods during the day. These three time slots collectively exhibited higher air pollutant concentrations. For instance, CO_2 emissions during these periods accounted for 17.94% and 18.71% of the total emissions, respectively. Conversely, emissions of air pollutants decrease significantly during the late evening and night-time hours. Between 22:00 and 06:00, the emissions accounted for only 5.32% of the total, representing the lowest emission levels. This reduction was primarily due to the complexity of night-time navigation, poor visibility, and the prioritisation of safety for passenger-focused ships. As a result, only a limited number of short-distance routes operated night services.

5.6.2. The Impact of Severe Weather on Emissions

The annual variation in pollutant emissions from passenger ships over time is shown in Figure 7. The changes in daily CO_2 emissions throughout the year are shown in Figure 8. Certain months exhibit outliers, with notable low-emission days such as August 4, August 25, September 1, and December 30. We hypothesised that these days were affected by severe

weather conditions, including typhoons, cold waves, strong winds, and high waves, which can significantly impact navigational visibility. Good visibility is critical for passenger ship navigation, as it enables crew members to accurately identify and follow channels, avoid obstacles, and adjust their course to ensure a safe and timely arrival at the destination. A statistical analysis of severe weather events in the Zhoushan region during 2020 was conducted, with the specific dates summarised in Tables 5 and 6. The timing of these severe weather events closely corresponded to the low-emission days. Typhoons and extreme cold wave conditions were found to have the most pronounced effects on the emissions.

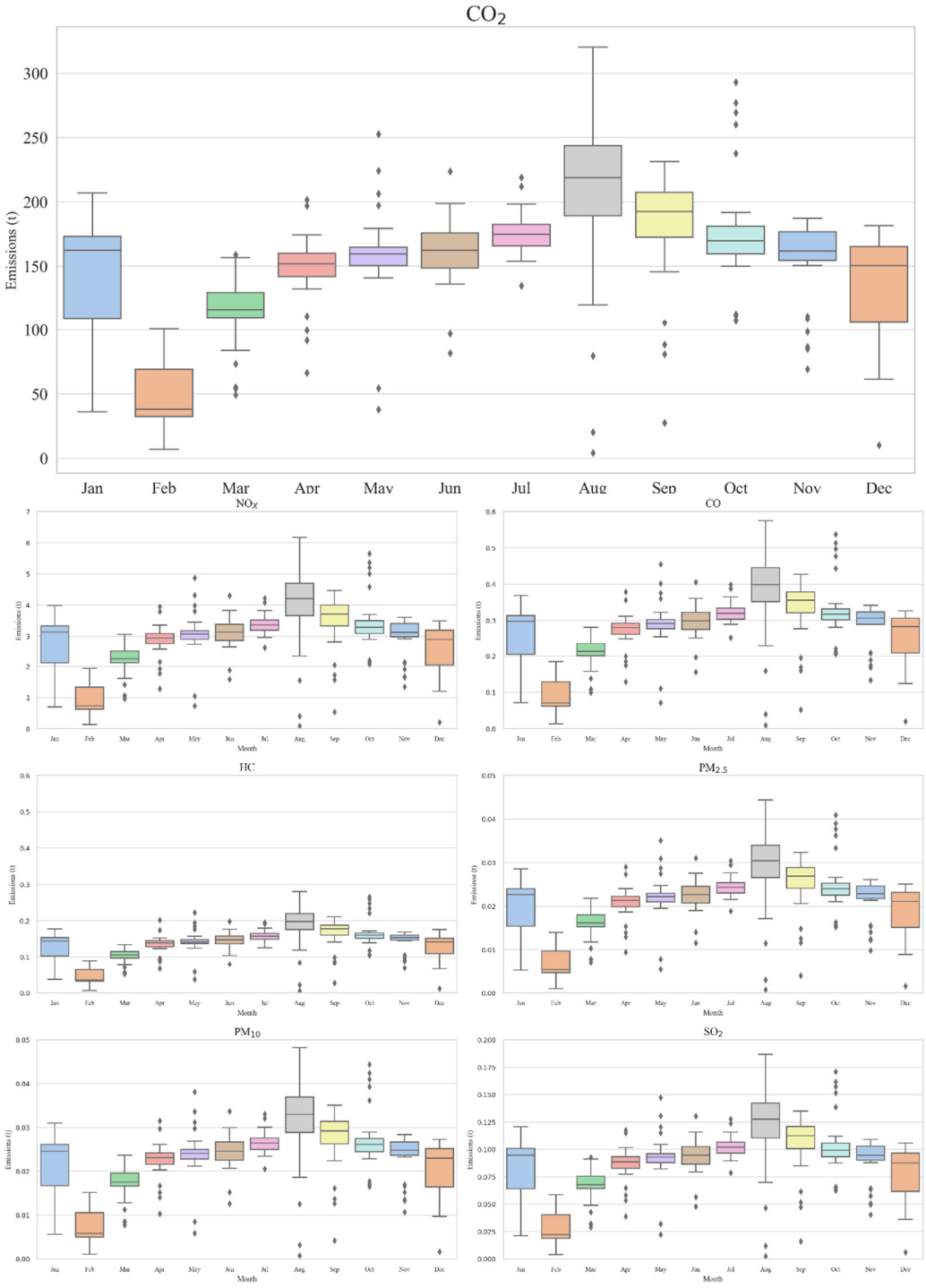

Figure 7. Annual emission distribution of each pollutant.

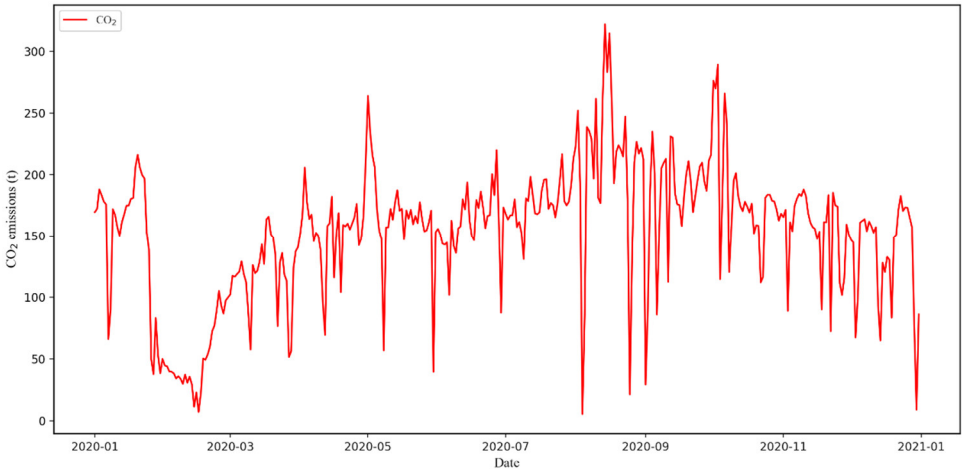

Figure 8. Daily changes in CO_2 emissions.

Table 5. Typhoons affecting Zhoushan area in 2020.

Typhoon No.	Name of the Typhoon	Date of Impact
2004	Hagupit	8.03–8.05
2008	Bavi	8.25–8.26
2009	Maysak	9.01–9.02
2010	Haishen	9.05–9.06

Table 6. Cold waves and gales affecting the Zhoushan area in 2020.

Type of Weather	Elapsed Time of Impact	Level of Warning
Cold wave	4.11–4.12	Severe
Cold wave	12.13–12.15	Moderate
Cold wave	12.28–12.30	Severe
Gale	1.22–1.28	Force 8–9
Gale	3.21	Force 8–11
Gale	4.12	Force 8–10
Gale	9.02–9.04	Force 8–11

During extreme weather events, such as typhoons, passenger ships often suspend operations, particularly in the typhoon-prone months of summer (e.g., August and September). While these suspensions reduce emissions on certain days, compensatory measures around the time of the extreme weather can lead to temporary fluctuations. For instance, after a typhoon, passenger ships may resume operations with increased voyages to recover the lost time, resulting in short-term emission surges. Similarly, some voyages are scheduled during brief weather windows when conditions permit, leading to detours to avoid typhoon paths or increased fuel consumption due to rough sea conditions. These factors collectively contribute to monthly emission outliers, where single-day or single-voyage CO_2 emissions were notably high. The combination of suspended operations during seasonal extreme weather and subsequent compensatory voyages results in significant variability in annual emissions.

5.6.3. Emissions from Different Types of Passenger Ships

The emissions data for different types of passenger ships are shown in Figure 9. The CO_2 emission patterns of the four ship types varied significantly, influenced by the seasonal demand and ship characteristics. Ro-Ro passenger ships exhibited the largest fluctuations in emissions, with their annual emissions ranging from 20 to 100 tons. These ships reach peak emissions during the summer tourism seasons, particularly in August, showing a strong correlation between peak emissions and seasonal demand. Ordinary passenger

ships had relatively stable emissions, ranging from 5 to 50 tons. While the emissions increased slightly during summer, the overall fluctuations were minimal, indicating balanced operational characteristics. Car–passenger ferries had the lowest emissions, ranging from approximately 0 to 7 tons. Their seasonal variation was minimal, and the difference between off-season and peak-season emissions was negligible, highlighting their low-emission and steady operational profile. High-speed passenger ships demonstrated significant emission variability, with peaks occurring in January, August, and December, reaching levels of up to 200 tons. This indicates their frequent use during peak passenger periods.

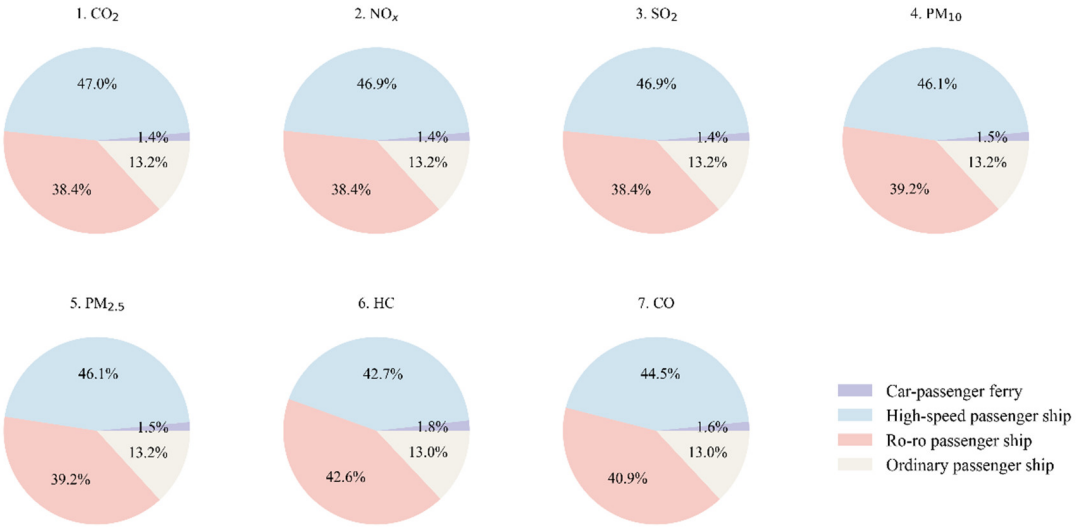

Figure 9. Percentage of emissions of each pollutant from different types of passenger ships.

Figure 9 also illustrates the contribution of each ship type to the pollutant emissions. High-speed passenger ships, which made up 31% of all passenger ships, accounted for 41.7% of the total main engine power and only 8.9% of the total tonnage, yet contributed the highest CO_2 emissions, amounting to 26,054.1 tons. This was largely due to their frequent activities, including multiple port arrivals and departures. Despite regulatory restrictions on night-time operations for high-speed passenger ships, their emissions remained notably high and warrant further attention. Ro-Ro passenger ships ranked second in emissions. Although their average main engine power is comparable to high-speed ships, they carry significantly more passengers and vehicles. With the largest total tonnage among the ship types, they contributed 38.4% of the CO_2 emissions. Ordinary passenger ships, with the highest passenger capacity and being primarily responsible for passenger transport, contributed only about 13.2% of the total CO_2 emissions. Car–passenger ferries had the lowest emissions, with a total CO_2 output of just 814.2 tons, reflecting their low environmental impact.

The similar HC emission contributions of high-speed passenger ships and Ro-Ro passenger ships may have been due to the commonality of the operating characteristics and fuel usage of the two types of ships. First, high-speed passenger ships and Ro-Ro passenger ships are usually equipped with similar medium speed diesel (MSD) engines, which tend to produce a higher proportion of unburned hydrocarbons (HCs) when operating at low loads. Although there were significant differences between the two types of ships in the emission of other pollutants such as CO_2 and NOx, HC emissions are more sensitive to changes in combustion efficiency. Incomplete engine combustion during low-load and idling operation will lead to increased HC emissions, which is a common operating condition during the berthing, unberthing, and low-speed sailing phases of high-speed passenger ships and Ro-Ro passenger ships.

5.7. Emissions from Different Operating Modes

Based on previous studies, the passenger ship emissions in the Zhoushan area were categorised into four operating modes (berthing, anchoring, unberthing, and cruising) to investigate the characteristics of the emissions under the different modes. The proportions of emissions from each mode are shown in Figure 10. The results indicated that, unlike other types of ships such as cargo ships, tankers, and fishing vessels, passenger ships generated 97% to 99% of their emissions during the cruising phase. This aligns with the operational characteristics of passenger ships, which spend most of their operational time in cruising mode and have relatively short anchoring durations. These findings are also consistent with the conclusions of Peng et al. [61]. It is hypothesised that, under normal circumstances, passenger ships powered by dual main engines shut off their engines when approaching passenger terminals. They rely on water currents, inertia, and their residual speed to reach the berth and wait for passengers to board and disembark. This operational behaviour differs from those of other ships entering and leaving ports, leading to especially low emissions during the berthing, anchoring, and unberthing phases.

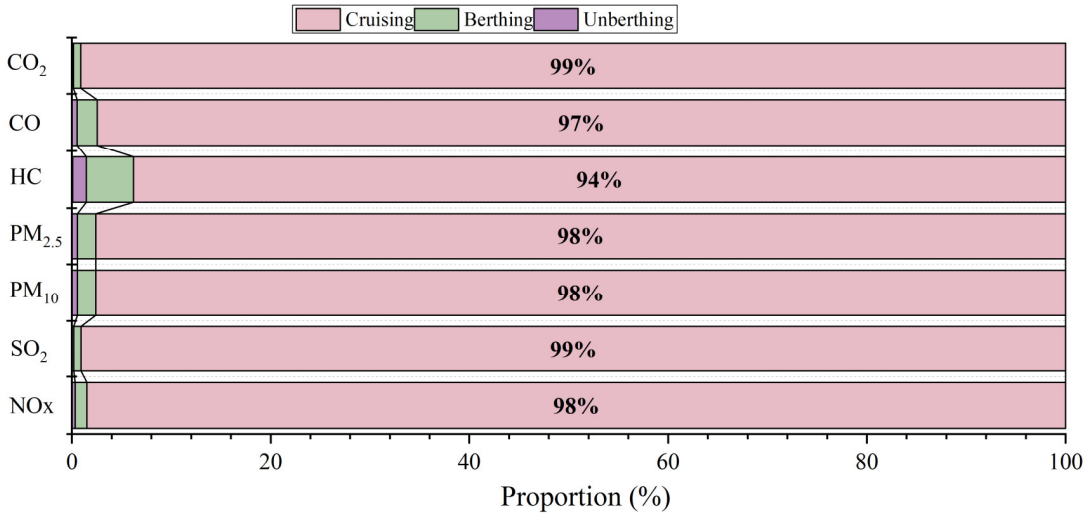

Figure 10. Proportion of emissions from passenger ships during different modes of operation.

5.8. Spatial Distribution

To analyse the spatial distribution of the exhaust emissions, a $0.002^\circ \times 0.002^\circ$ grid was created to rasterise the study area. Based on the geographic coordinates in the AIS data, all the pollutant emissions from passenger ships in the region were aggregated and allocated to the corresponding grid cells. The results are shown in Figure 11.

The spatial distribution of the emissions exhibited clear patterns that correspond to the ships' navigation routes. The emissions along the routes between Daishan Island, Qushan Island, and the Shengsi Archipelago were significantly higher than in other areas. Similarly, there was notable activity on the routes connecting Zhoushan Island with Liuheng Island, Xiazhi Island, and Taohua Island. It is important to note that most passenger ship emissions occurred within designated navigation areas. This can be explained by the nature of passenger ship operations, which primarily serve passenger transport, tourism, and leisure purposes. Before routes are launched, passenger ships will undergo safety risk assessments to ensure compliance with safety requirements. Ships are permitted to only operate in waters that meet passenger safety standards, using routes recommended or designated by administrative authorities, and embark/disembark passengers at designated terminals. In the Zhoushan area, which is crowded with various commercial and fishing vessels, adhering to fixed routes helps reduce the risk of ship collisions and ensures the safety of the passengers onboard.

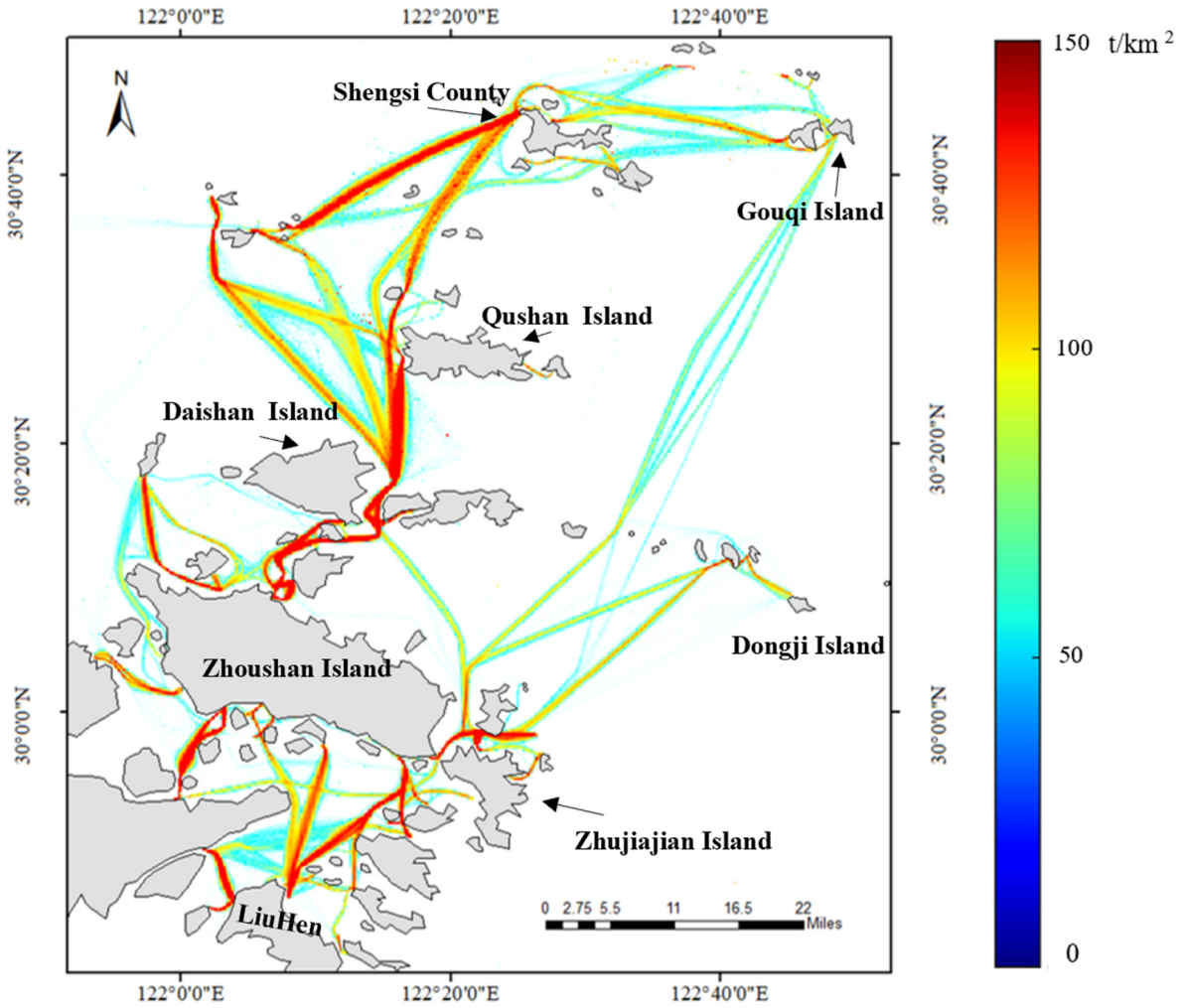

Figure 11. Spatial distribution of annual CO_2 passenger ship emissions.

5.9. Proposed Emission Reduction Measures

Based on the findings of this study, several practical measures can be proposed to reduce emissions from maritime activities. These measures, supported by accurate emissions calculations, could significantly mitigate environmental impacts:

1. Route Optimisation: By analysing vessel traffic patterns and emission hotspots, route optimisation can help minimise unnecessary travel and reduce fuel consumption. Advanced navigation systems and predictive algorithms can identify the most energy-efficient paths, avoiding congested or high-emission zones. This approach not only reduces emissions but also improves operational efficiency.
2. Speed Reduction Programs (Slow Steaming): Lowering vessel speeds, especially in emission-sensitive or congested areas, can significantly reduce fuel consumption and emissions.
3. Training and Awareness Programs: Educating ship operators and crews about energy-efficient practices, such as optimal engine operation and maintenance, can improve compliance and operational efficiency. Awareness programs can highlight the environmental and economic benefits of adopting sustainable practices.

While these measures represent actionable strategies, their successful implementation depends on integrating emissions data into decision-making frameworks. For instance, the granular emission calculations presented in this study can identify high-impact areas for policy intervention or guide investments in cleaner technologies. Future research could

explore the cost-effectiveness and practical barriers associated with these measures to provide comprehensive guidance for policymakers and industry stakeholders

6. Conclusions

This study analysed pollutant emissions from short-distance passenger ships in the Zhoushan Archipelago from January to December 2020 using high-resolution AIS data. The analysis incorporated various meteorological factors and detailed passenger ship specifications, employing the bottom–up approach to comprehensively investigate the emission characteristics of passenger ships of different types.

The results indicate that the activity-based bottom–up approach is suitable for analysing frequently operating passenger ships. During the selected timeframe, the total emissions of CO_2, NO_x, CO, $PM_{2.5}$, PM_{10}, SO_2, and HCs were calculated to be 54,895.75 tons, 1057.82 tons, 101.46 tons, 7.68 tons, 8.33 tons, 32.02 tons, and 50.34 tons, respectively. High-speed passenger ships accounted for the highest proportion of the emissions, accounting for approximately 42.1–46.8%, followed by Ro-Ro passenger ships at 37.7–42.2%. The emissions from ordinary passenger ships and car–passenger ferries were relatively lower, contributing 13.8–14.2% and 1.3–1.7%, respectively. When comparing the emissions across different operating modes, cruising accounted for the largest share of pollutant emissions, with the other stages (berthing, anchoring, and manoeuvring) contributing only 1–3%. This was attributed to the unique operational characteristics of passenger ships. The two primary activity areas for passenger ships were between Zhoushan Island, Daishan Island, and the Qushan Archipelago, and between Liuheng Island, Xiazhi Island, and the Taohua Archipelago. These two regions saw the highest emissions due to the frequency of passenger ship activities.

This study utilised high-precision ship attribute data, addressing issues in traditional emission calculations such as inaccuracies related to meteorological factors and main engine power deviations. The findings demonstrate that passenger ship emissions follow a discernible pattern. Clarifying activity-based emission characteristics is crucial for regulatory authorities to formulate effective emission reduction strategies and serves as a reference for passenger transport companies in managing emissions. Additionally, it indirectly supports low-carbon and energy-saving practices in ports, enhancing the resilience of future port and marine environmental management.

However, this study has certain limitations. When applying the model to other regions, the availability of foundational data remains a constraint. Although regulatory authorities mandate that passenger ships use fuel with a sulphur content not exceeding 0.5%, discrepancies between requirements and actual implementation may lead to underestimations of SO_2 emissions. Furthermore, it is challenging to accurately obtain per-voyage fuel consumption data. Future research integrating voyage-specific fuel consumption data could provide a more reliable method for improving precision.

Author Contributions: X.X.: Conception and design of the study, data analysis, interpretation of results, manuscript writing; X.L.: Data collection, data interpretation; L.F.: Literature search, manuscript revision; W.Y.Y.: Statistical analysis, manuscript revision; H.F.: Study design and guidance. All authors have read and agreed to the published version of the manuscript.

Funding: This work was sponsored by K.C. Wong Magna Fund in Ningbo University, China and 111 Project [grant number D21013].

Institutional Review Board Statement: Not applicable.

Informed Consent Statement: Not applicable.

Data Availability Statement: The raw data supporting the conclusions of this article will be made available by the authors on request.

Conflicts of Interest: The authors declare no conflict of interest.

References

1. Wang, L.; Li, Y. Estimation methods and reduction strategies of port carbon emissions-what literatures say? *Mar. Pollut. Bull.* **2023**, *195*, 115451. [CrossRef] [PubMed]
2. Ytreberg, E.; Åström, S.; Fridell, E. Valuating environmental impacts from ship emissions–The marine perspective. *J. Environ. Manag.* **2021**, *282*, 111958. [CrossRef]
3. Kose, S.; Sekban, D. Emphasizing the importance of using cold-ironing technology by determining the share of hotelling emission value within the total emission. *Transp. Saf. Environ.* **2022**, *4*, tdac010. [CrossRef]
4. Gray, N.; McDonagh, S.; O'Shea, R.; Smyth, B.; Murphy, J.D. Decarbonising ships, planes and trucks: An analysis of suitable low-carbon fuels for the maritime, aviation and haulage sectors. *Adv. Appl. Energy* **2021**, *1*, 100008. [CrossRef]
5. Chen, X.; Zheng, J.; Li, C.; Wu, B.; Wu, H.; Montewka, J. Maritime traffic situation awareness analysis via high-fidelity ship imaging trajectory. *Multimed. Tools Appl.* **2024**, *83*, 48907–48923. [CrossRef]
6. Shang, W.-L.; Zhang, J.; Wang, K.; Yang, H.; Ochieng, W. Can financial subsidy increase electric vehicle (EV) penetration---evidence from a quasi-natural experiment. *Renew. Sustain. Energy Rev.* **2024**, *190*, 114021. [CrossRef]
7. Van Roy, W.; Merveille, J.-B.; Van Nieuwenhove, A.; Scheldeman, K.; Maes, F. Policy recommendations for international regulations addressing air pollution from ships. *Mar. Policy* **2024**, *159*, 105913. [CrossRef]
8. Liu, J.; Jiang, X.; Huang, W.; He, Y.; Yang, Z. A novel approach for navigational safety evaluation of inland waterway ships under uncertain environment. *Transp. Saf. Environ.* **2022**, *4*, tdab029. [CrossRef]
9. Kumar, P.; Beig, G.; Sahu, S.; Yadav, R.; Maji, S.; Singh, V.; Bamniya, B. Development of a high-resolution emissions inventory of carbonaceous particulate matters and their growth during 2011–2018 over India. *Atmos. Environ.* **2023**, *303*, 119750. [CrossRef]
10. Zhang, K.; Lin, Q.; Lian, F.; Feng, H. Estimating emissions from fishing vessels: A big Beidou data analytical approach. *Front. Mar. Sci.* **2024**, *11*, 1418366. [CrossRef]
11. Zhai, J.; Yu, G.; Zhang, J.; Shi, S.; Yuan, Y.; Jiang, S.; Xing, C.; Cai, B.; Zeng, Y.; Wang, Y. Impact of ship emissions on air quality in the Greater Bay Area in China under the latest global marine fuel regulation. *Environ. Sci. Technol.* **2023**, *57*, 12341–12350. [CrossRef] [PubMed]
12. Han, Y.; Ma, W.; Ma, D. Green maritime: An improved quantum genetic algorithm-based ship speed optimization method considering various emission reduction regulations and strategies. *J. Clean. Prod.* **2023**, *385*, 135814. [CrossRef]
13. IMO. *Guidelines for the Installation of a Shipborne Automatic Identification System (AIS)*; International Maritime Organization: London, UK, 2002.
14. Nunes, R.; Alvim-Ferraz, M.; Martins, F.; Sousa, S. The activity-based methodology to assess ship emissions-A review. *Environ. Pollut.* **2017**, *231*, 87–103. [CrossRef] [PubMed]
15. You, Y.; Lee, J.C. Activity-based evaluation of ship pollutant emissions considering ship maneuver according to transportation plan. *Int. J. Nav. Archit. Ocean. Eng.* **2022**, *14*, 100427. [CrossRef]
16. Tzannatos, E. Ship emissions and their externalities for Greece. *Atmos. Environ.* **2010**, *44*, 2194–2202. [CrossRef]
17. Corbett, J.J.; Koehler, H.W. Updated emissions from ocean shipping. *J. Geophys. Res. Atmos.* **2003**, *108*, 4650. [CrossRef]
18. Chen, X.; Liu, S.; Liu, R.W.; Wu, H.; Han, B.; Zhao, J.J.O. Quantifying Arctic oil spilling event risk by integrating an analytic network process and a fuzzy comprehensive evaluation model. *Ocean. Coast. Manag.* **2022**, *228*, 106326. [CrossRef]
19. Chen, X.; Xian, J.; Liu, S.; Zhao, J.; Wu, H.; Montewka, J. Autonomous port management based AGV path planning and optimization via an ensemble reinforcement learning framework. *Ocean. Coast. Manag.* **2024**, *251*, 107087. [CrossRef]
20. Li, Y.; Zhang, Y.; Cheng, J.; Zheng, C.; Li, M.; Xu, H.; Wang, R.; Chen, D.; Wang, X.; Fu, X.; et al. Comparative Analysis, Use Recommendations, and Application Cases of Methods for Develop Ship Emission Inventories. *Atmosphere* **2022**, *13*, 1224. [CrossRef]
21. Jalkanen, J.-P.; Brink, A.; Kalli, J.; Pettersson, H.; Kukkonen, J.; Stipa, T. A modelling system for the exhaust emissions of marine traffic and its application in the Baltic Sea area. *Atmos. Chem. Phys.* **2009**, *9*, 9209–9223. [CrossRef]
22. Winther, M.; Christensen, J.H.; Plejdrup, M.S.; Ravn, E.S.; Eriksson, Ó.F.; Kristensen, H.O. Emission inventories for ships in the arctic based on satellite sampled AIS data. *Atmos. Environ.* **2014**, *91*, 1–14. [CrossRef]
23. Goldsworthy, L.; Goldsworthy, B. Modelling of ship engine exhaust emissions in ports and extensive coastal waters based on terrestrial AIS data–An Australian case study. *Environ. Model. Softw.* **2015**, *63*, 45–60. [CrossRef]
24. Pokhrel, R.; Lee, H. Estimation of air pollution from the OGVs and its dispersion in a coastal area. *Ocean. Eng.* **2015**, *101*, 275–284. [CrossRef]

25. Zhou, C.; Huang, H.; Liu, Z.; Ding, Y.; Xiao, J.; Shu, Y. Identification and analysis of ship carbon emission hotspots based on data field theory: A case study in Wuhan Port. *Ocean. Coast. Manag.* **2023**, *235*, 106479. [CrossRef]
26. Chen, D.; Wang, X.; Li, Y.; Lang, J.; Zhou, Y.; Guo, X.; Zhao, Y. High-spatiotemporal-resolution ship emission inventory of China based on AIS data in 2014. *Sci. Total Environ.* **2017**, *609*, 776–787. [CrossRef] [PubMed]
27. Toscano, D.; Murena, F.; Quaranta, F.; Mocerino, L. Assessment of the impact of ship emissions on air quality based on a complete annual emission inventory using AIS data for the port of Naples. *Ocean. Eng.* **2021**, *232*, 109166. [CrossRef]
28. Ye, J.; Chen, J.; Wen, H.; Wan, Z.; Tang, T. Emissions assessment of bulk carriers in China's east Coast-Yangtze River maritime network based on different shipping modes. *Ocean. Eng.* **2022**, *249*, 110903. [CrossRef]
29. Li, H.; Jia, P.; Wang, X.; Yang, Z.; Wang, J.; Kuang, H. Ship carbon dioxide emission estimation in coastal domestic emission control areas using high spatial-temporal resolution data: A China case. *Ocean. Coast. Manag.* **2023**, *232*, 106419. [CrossRef]
30. Zhi, G.; Du, J.; Chen, A.; Jin, W.; Ying, N.; Huang, Z.; Xu, P.; Wang, D.; Ma, J.; Zhang, Y. Progression of an emission inventory of China integrating CO_2 with air pollutants: A chance to learn the influence of development on emissions. *Atmos. Environ.* **2024**, *316*, 120184. [CrossRef]
31. Orlandi, A.; Calastrini, F.; Kalikatzarakis, M.; Guarnieri, F.; Busillo, C.; Coraddu, A. Air quality forecasting of along-route ship emissions in realistic meteo-marine scenarios. *Ocean. Eng.* **2024**, *291*, 116464. [CrossRef]
32. Moreno-Gutiérrez, J.; Durán-Grados, V. Calculating ships' real emissions of pollutants and greenhouse gases: Towards zero uncertainties. *Sci. Total Environ.* **2021**, *750*, 141471. [CrossRef] [PubMed]
33. Carić, H.; Klobučar, G.; Štambuk, A. Ecotoxicological risk assessment of antifouling emissions in a cruise ship port. *J. Clean. Prod.* **2016**, *121*, 159–168. [CrossRef]
34. Dragović, B.; Tzannatos, E.; Tselentis, V.; Meštrović, R.; Škurić, M. Ship emissions and their externalities in cruise ports. *Transp. Res. Part D: Transp. Environ.* **2018**, *61*, 289–300. [CrossRef]
35. Chen, Q.; Lau, Y.-Y.; Ge, Y.-E.; Dulebenets, M.A.; Kawasaki, T.; Ng, A.K. Interactions between Arctic passenger ship activities and emissions. *Transp. Res. Part D Transp. Environ.* **2021**, *97*, 102925. [CrossRef]
36. Chen, Q.; Ge, Y.-E.; Lau, Y.-Y.; Dulebenets, M.A.; Sun, X.; Kawasaki, T.; Mellalou, A.; Tao, X. Effects of COVID-19 on passenger shipping activities and emissions: Empirical analysis of passenger ships in Danish waters. *Marit. Policy Manag.* **2023**, *50*, 776–796. [CrossRef]
37. Huang, H.; Zhou, C.; Xiao, C.; Huang, L.; Wen, Y.; Wang, J.; Peng, X. Effect of seasonal flow field on inland ship emission assessment: A case study of ferry. *Sustainability* **2020**, *12*, 7484. [CrossRef]
38. Chou, C.-C.; Hsu, H.-P.; Wang, C.-N.; Yang, T.-L. Analysis of energy efficiencies of in-port ferries and island passenger-ships and improvement policies to reduce CO_2 emissions. *Mar. Pollut. Bull.* **2021**, *172*, 112826. [CrossRef] [PubMed]
39. Mannarini, G.; Salinas, M.L.; Carelli, L.; Fassò, A. How COVID-19 affected GHG emissions of ferries in Europe. *Sustainability* **2022**, *14*, 5287. [CrossRef]
40. Baird, A.J.; Pedersen, R.N. Analysis of CO_2 emissions for island ferry services. *J. Transp. Geogr.* **2013**, *32*, 77–85. [CrossRef]
41. Cooper, D. Exhaust emissions from high speed passenger ferries. *Atmos. Environ.* **2001**, *35*, 4189–4200. [CrossRef]
42. Mojarrad, M.; Thorne, R.J.; Rødseth, K.L. Technical and cost analysis of zero-emission high-speed ferries: Retrofitting from diesel to green hydrogen. *Heliyon* **2024**, *10*, e27479. [CrossRef] [PubMed]
43. Zhou, C.; Tang, W.; Ding, Y.; Huang, H.; Xu, H. Analysis of Carbon Emission Reduction Paths for Ships in the Yangtze River: The Perspective of Alternative Fuels. *J. Mar. Sci. Eng.* **2024**, *12*, 947. [CrossRef]
44. Chen, X.; Chen, W.; Wu, B.; Wu, H.; Xian, J. Ship visual trajectory exploitation via an ensemble instance segmentation framework. *Ocean. Eng.* **2024**, *313*, 119368. [CrossRef]
45. Shang, W.-L.; Chen, Y.; Yu, Q.; Song, X.; Chen, Y.; Ma, X.; Chen, X.; Tan, Z.; Huang, J.; Ochieng, W. Spatio-temporal analysis of carbon footprints for urban public transport systems based on smart card data. *Appl. Energy* **2023**, *352*, 121859. [CrossRef]
46. Mao, J.; Zhang, Y.; Yu, F.; Chen, J.; Sun, J.; Wang, S.; Zou, Z.; Zhou, J.; Yu, Q.; Ma, W. Simulating the impacts of ship emissions on coastal air quality: Importance of a high-resolution emission inventory relative to cruise-and land-based observations. *Sci. Total Environ.* **2020**, *728*, 138454. [CrossRef] [PubMed]
47. Chen, D.; Zhao, Y.; Nelson, P.; Li, Y.; Wang, X.; Zhou, Y.; Lang, J.; Guo, X. Estimating ship emissions based on AIS data for port of Tianjin, China. *Atmos. Environ.* **2016**, *145*, 10–18. [CrossRef]
48. Chen, S.; Wang, F.; Wei, X.; Tan, Z.; Wang, H.J.T.R.R. Analysis of tugboat activities using AIS data for the Tianjin port. *Transp. Res. Rec. J. Transp. Res. Board* **2020**, *2674*, 498–509. [CrossRef]
49. Tian, Y.; Ren, L.; Wang, H.; Li, T.; Yuan, Y.; Zhang, Y. Impact of AIS data thinning on ship air pollutant emissions inventories. *Atmosphere* **2022**, *13*, 1135. [CrossRef]
50. Chen, X.; Yang, J. Analysis of the uncertainty of the AIS-based bottom-up approach for estimating ship emissions. *Mar. Pollut. Bull.* **2024**, *199*, 115968. [CrossRef]
51. Shu, Y.; Hu, A.; Zheng, Y.; Gan, L.; Xiao, G.; Zhou, C.; Song, L. Evaluation of ship emission intensity and the inaccuracy of exhaust emission estimation model. *Ocean. Eng.* **2023**, *287*, 115723. [CrossRef]

52. Grigoriadis, A.; Mamarikas, S.; Ioannidis, I.; Majamäki, E.; Jalkanen, J.-P.; Ntziachristos, L. Development of exhaust emission factors for vessels: A review and meta-analysis of available data. *Atmos. Environ. X* **2021**, *12*, 100142. [CrossRef]
53. Limited, E.U. *Quantification of Emissions from Ships Associated with Ship Movements Between Ports in the European Community*; European Commission: Brussels, Belgium, 2002.
54. Group, S.C. Port of Los Angeles Inventory of Air Emissions-2012. 2013. Available online: https://kentico.portoflosangeles.org/getmedia/6cbdfeec-49c0-4758-b2b0-8fab74a79578/2012_Air_Emissions_Inventory (accessed on 3 March 2024).
55. Fu, Q.; Shen, Y.; Zhang, J. On the ship pollutant emission inventory in Shanghai port. *J. Saf. Environ.* **2012**, *12*, 57–64.
56. Zhao, J.; Zhang, Y.; Patton, A.P.; Ma, W.; Kan, H.; Wu, L.; Fung, F.; Wang, S.; Ding, D.; Walker, K. Projection of ship emissions and their impact on air quality in 2030 in Yangtze River delta, China. *Environ. Pollut.* **2020**, *263*, 114643. [CrossRef] [PubMed]
57. Huang, L.; Wen, Y.; Geng, X.; Zhou, C.; Xiao, C. Integrating multi-source maritime information to estimate ship exhaust emissions under wind, wave and current conditions. *Transp. Res. Part D Transp. Environ.* **2018**, *59*, 148–159. [CrossRef]
58. Chen, S.; Meng, Q.; Jia, P.; Kuang, H. An operational-mode-based method for estimating ship emissions in port waters. *Transp. Res. Part D Transp. Environ.* **2021**, *101*, 103080. [CrossRef]
59. Lin, Q.; Yin, B.; Zhang, X.; Grifoll, M.; Feng, H. Evaluation of ship collision risk in ships' routeing waters: A Gini coefficient approach using AIS data. *Phys. A Stat. Mech. Its Appl.* **2023**, *624*, 128936. [CrossRef]
60. Feng, H.; Grifoll, M.; Yang, Z.; Zheng, P. Collision risk assessment for ships' routeing waters: An information entropy approach with Automatic Identification System (AIS) data. *Ocean. Coast. Manag.* **2022**, *224*, 106184. [CrossRef]
61. Peng, X.; Ding, Y.; Yi, W.; Laroussi, I.; He, T.; He, K.; Liu, H. The inland waterway ship emission inventory modeling: The Yangtze River case. *Transp. Res. Part D Transp. Environ.* **2024**, *129*, 104138. [CrossRef]